A solid oxide fuel cell fuelled by methane recovered from groundwater

Saadabadi, S. Ali; van Linden, Niels; Heinsbroek, Abel; Aravind, P. V.

DOI
10.1016/j.jclepro.2021.125877

Publication date
2021

Document Version
Final published version

Published in
Journal of Cleaner Production

Citation (APA)
Saadabadi, S. A., van Linden, N., Heinsbroek, A., & Aravind, P. V. (2021). A solid oxide fuel cell fuelled by methane recovered from groundwater. *Journal of Cleaner Production*, *291*, Article 125877. https://doi.org/10.1016/j.jclepro.2021.125877

Journal of Cleaner Production 291 (2021) 125877

Contents lists available at ScienceDirect

Journal of Cleaner Production

journal homepage: www.elsevier.com/locate/jclepro

A solid oxide fuel cell fuelled by methane recovered from groundwater

S. Ali Saadabadi [a, *], Niels van Linden [b], Abel Heinsbroek [c], P.V. Aravind [a]

[a] Delft University of Technology, Faculty of 3ME, Department of Process and Energy, Leeghwaterstraat 39, 2628 CB, Delft, the Netherlands
[b] Delft University of Technology, Faculty of Civil Engineering and Geosciences, Department of Water Management, Stevinweg 1, 2628 CN, Delft, the Netherlands
[c] Vitens N.V., Oude Veerweg 1, Postbus 1205, 8001 BE, Zwolle, the Netherlands

ARTICLE INFO

Article history:
Received 2 October 2020
Received in revised form
28 December 2020
Accepted 5 January 2021
Available online 7 January 2021

Handling editor: Mingzhou Jin

Keywords:
Groundwater
Resource recovery
Drinking water
Methane
Energy generation
Solid oxide fuel cell

ABSTRACT

This study investigates the feasibility of electricity production in a solid oxide fuel cell using methane recovered from groundwater as the fuel. Methane must be removed from groundwater for the production of drinking water to, amongst others, avoid bacterial regrowth. Instead of releasing methane to the atmosphere or converting it to carbon dioxide by flaring, methane can also be recovered by vacuum stripping and served as a fuel. However, the electrical efficiency of currently used combustion-based technologies fuelled with methane-rich gas is limited to 35% due to the low heating value of the recovered gas (70 mol. % methane) and power derating due to the presence of carbon dioxide (25 mol.%). We propose to use a solid oxide fuel cell to use the methane-rich gas as fuel. Solid Oxide Fuel Cells are fuel-flexible and potentially attain higher electrical efficiencies up to 60%. To this end, specific gas processing, including cleaning and methane reforming, is required to allow for durable operation in a solid oxide fuel cell. We assessed whether electricity could be generated by a solid oxide fuel cell using methane recovered from a full-scale drinking water treatment plant as a fuel. The groundwater had a methane concentration of 45 $mg \cdot L^{-1}$, and the recovered gas by vacuum towers contained 70 mol% methane. We used a gas cleaning reactor with impregnated activated carbon to remove hydrogen sulfide traces from the methane-rich gas. Thermodynamic calculations showed that additional steam is required to achieve a high methane reforming. The added steam and the carbon dioxide content in the recovered gas simultaneously contribute to the methane reforming to prevent carbon deposition. The measured open circuit potential corresponded with the theoretical Nernst voltage, implying high methane reforming in the solid oxide fuel cell. The achieved power density of the cell fuelled with the methane-rich gas (mixed with steam) was 27% less than the hydrogen-fuelled cell. Ultimately, 51.2% of the power demand of the plant can be covered by replacing the gas engine in a drinking water treatment with a 915 kW solid oxide fuel cell system fuelled by the methane recovered from the groundwater, while the greenhouse gas emission can be reduced by 17.6%.

1. Introduction

1.1. Groundwater as a source of drinking water

Groundwater is the most frequently used source for the production of drinking water in the Netherlands (Vewin, 2019). However, treatment of groundwater is needed to produce drinking water to meet the guidelines for drinking water set by the Drinking Water Directive (Council Directive 98/83/EC) in Europe. The required treatment depends on the specific composition of the groundwater, which amongst others depends on the characteristics of the subsurface. In addition to the conventional removal of natural organic matter, hardness, nitrate, and other geogenous substances, recent trends in drinking water production from groundwater focus on the removal of organic micropollutants (Lapworth et al., 2012) and toxic metals such as arsenic (Ahmad et al., 2020). Furthermore, drinking water treatment plants (DWTPs) must minimise their carbon footprint to meet the 2020 Climate and Energy Package and the 2030 Climate and Energy Framework set by the European Union by decreasing the consumption of energy and chemicals and the direct emission of greenhouse gases (EurEau, 2019).

* Corresponding author.
E-mail address: s.a.saadabadi@tudelft.nl (S.A. Saadabadi).

https://doi.org/10.1016/j.jclepro.2021.125877

1.2. Removal of methane from groundwater

Besides the presence of natural organic matter, carbon can be present in groundwater as methane (CH_4), which must be removed to avoid bacterial regrowth during the treatment, transportation, and drinking water distribution. CH_4 becomes present in groundwater as a result of anaerobic degradation of organic matter in the subsurface or the infiltration of CH_4 from natural gas reservoirs (Osborn et al., 2011). Traditional treatment of groundwater typically comprises aeration using tower- and plate-aerators and cascades, to add oxygen (O_2) to the water and simultaneously strip undesired gases, such as hydrogen sulphide (H_2S), carbon dioxide (CO_2), and CH_4. However, the application of aeration results in greenhouse gas emissions to the environment because the off-gas containing air and the undesired gases are directly emitted. The emission of CH_4 is undesirable because it has 28 times higher global warming potential than CO_2 (Stocker et al., 2013). The annual methane emissions by the groundwater treatment global sector was estimated to be 0.53 Tg which is around 0.2% of global methane emissions (Kulongoski and Mcmahon, 2019). Therefore, the emission of CH4 during groundwater treatment can contribute significantly to the total carbon footprint of DWTPs.

Besides aeration, CH_4 can be removed from water by vacuum (membrane) stripping (Velasco et al., 2018), through which a gas with a concentration of CH_4 of 60% can be recovered from wastewater effluents (Rongwong et al., 2018). The recovery of CH_4 by vacuum (membrane) stripping allows for flaring of CH_4, resulting in the conversion of CH_4 to CO_2, lowering the carbon footprint. However, the direct emission to the environment and the flaring of CH4 both ignore the potential to generate energy after the recovery of CH_4.

1.3. Energy generation from recovered methane

Recent efforts to valorise recovered CH_4 from water showed that it is possible to recover CH_4 for energy generation in a (micro) gas turbine (Rongwong et al., 2018). Combustion-based energy conversion technologies, such as gas turbines, are widely applied to generate electricity and heat from (recovered) CH_4. However, combustion-based energy conversion technologies emit a large amount of CO_2 (per kW electrical power generation) and have an electrical efficiency of 20–35% (Trendewicz and Braun, 2013), while micro-scale systems (<10 kWe) only have an electrical efficiency of 20% (Mikalsen et al., 2009).

On the contrary, electrochemical energy conversion technologies, such as solid oxide fuel cells (SOFCs), are reported to have an electrical efficiency up to 60% when using CH_4 as fuel, while the total energy efficiency can go up to 90% when the generated high-grade heat is used (Stambouli and Traversa, 2002). More specifically, Farhad et al. (2010) achieved an electrical efficiency of 42% for a 1 kWe SOFC stack with an external steam reforming process, fuelled with biogas (60 mol.% CH_4 and 35 mol.% CO_2) mixed with anode off-gas. Tjaden et al. (2014) achieved a 57% electrical efficiency for a 25 kWe SOFC system using biogas fuel. Both studies used biogas containing around 60% CH_4, while Staniforth and Ormerod (2003) showed the feasibility of using biogas containing only 45% of CH_4 as a fuel for an SOFC. Furthermore, Yi et al. (2005) showed that the efficiency of the SOFC decreases only by 1% when shifting from natural gas (CH_4 > 90%) to biogas (with a system efficiency of 51.1%) as the primary source of CH_4. Hence, SOFCs are very flexible with respect to fuel composition in contrast to combustion-based technologies, opening opportunities for more efficient energy generation from fuels recovered from (waste) water.

1.4. Methane processing for energy generation in SOFCs

SOFCs are considered to be fuel-flexible fuel cells because besides hydrogen (H_2), also carbon monoxide (CO) can directly electrochemically react with oxygen ions (O^{2-}). To allow for O^{2-} transport through the solid electrolyte in SOFCs, operational temperatures of 600–900 °C must be maintained. Typically, nickel is used to catalyse the oxidation of H_2 at the anode (Mahato et al., 2015). However, SOFCs do not rely on the direct electrochemical oxidation of CH_4 (Staniforth and Ormerod, 2003). Therefore, to use CH_4 as a fuel, it must be reformed, either externally or in-situ (internal) at the anode, resulting in the generation of H_2 and CO. Reforming of CH_4 can generally be achieved by dry reforming (Eq. 1), steam reforming (Eq. 2) and partial oxidation, which are extensively discussed in the reviews of Gür (2016).

Steam (i.e., water vapor) and CO_2 are often already present in the fuel when CH_4 is recovered from the water, allowing for in-situ CH_4 reforming at the anode, since a suitable nickel catalyst is already present at the anode (Fan et al., 2015). However, a challenge during the reforming of CH_4 is the deposition of carbon, which is also catalysed by nickel at temperatures above 450 °C (Girona et al., 2012). Carbon deposition decreases the cell catalytic properties and causes anode structure damage due to local thermal stresses, leading to delamination of the anode material (Chen et al., 2011). To guarantee a durable and efficient SOFC operation, precise CH_4 reforming is required because high concentrations of reforming agents (steam and CO_2) influence the SOFC performance by decreasing the electric potential. Furthermore, the H_2 and CO concentrations change based on water gas shift reaction at equilibrium condition (Eq. 3), which also impacts the electric potential. The optimal reforming process depends on the actual gas composition of the CH_4-rich gas since direct dry reforming or steam reforming can be achieved when the required amount of CO_2 or water, respectively, is already present in the gas.

Dry CH_4 Reforming :

$$CH_4 + CO_2 \leftrightarrow 2H_2 + 2CO\ ,\ \Delta H^0_{T=298} = 247\ kJ.mol^{-1} \quad (1)$$

Steam CH_4 Reforming:

$$CH_4 + H_2O \leftrightarrow 3H_2 + CO\ ,\ \Delta H^0_{T=298} = 206\ kJ.mol^{-1} \quad (2)$$

Water Gas Shift Reaction:

$$CO + H_2O \leftrightarrow H_2 + CO_2\ ,\ \Delta H^0_{T=298} = -41\ kJ.mol^{-1} \quad (3)$$

1.5. Removal of contaminants for fuel cell

When CH_4 is recovered from the water, for example, after biogas production during waste (water) treatment, contaminations like H_2S can be present in the recovered fuel. H_2S is a corrosive gas that could form concentrated sulphuric acid, depending on humidity, O_2 concentration and the presence of bio-film. It can lead to the deterioration of pipelines and other metal equipment (Zhou et al., 2013). Equipment in conventional power generation systems can tolerate H_2S levels around 250 ppm (Abatzoglou and Boivin, 2009). Contaminants such as H_2S and hydrochloric acids strongly influence the SOFC performance and the durability of the cells (Papadias et al., 2012).

H_2S deactivates the nickel catalyst present on the anode by forming nickel sulphide particles on the anode surface. The formation of large and dense nickel sulphide particles leads to a decrease in the three-phase boundaries (where the electrochemical

reactions take place) (Sasaki et al., 2011). A detailed kinetic model of methane reforming has been developed by Appari et al. (2014). The results showed an immediate deactivation of the catalyst at the introduction of H_2S as a result of the occupation of the Ni-surface by sulfur. The impact of sulfur poisoning on cell performance of different SOFC anodes have illustrated that Ni/GDC (Gadolinium Doped Ceria) cermet (ceramic-metallic composite) anode has a better performance during the exposure to H_2S-containing hydrogen fuels (Zhang et al., 2010). This is due to the fact that GDC possesses mixed ionic and electronic conductivity (Ouweltjes et al., 2006) studied the influence of sulfur contaminant (2–9 ppm) on the Ni-GDC cell. Results indicated that sulfur mainly impacts the methane reforming while the effect was negligible for H_2 and CO electrochemical oxidation. Experimental studies on conventional SOFC anode (Ni-SSZ) showed considerable electric potential drops with H_2S impurities higher than 5 ppm in the fuel (Sasaki et al., 2007). (Bao et al., 2009) have reported a rapid cell voltage drop after exposure to H_2S, which is reversible after short-term exposure to a 1 ppm H_2S. Even though SOFCs are known as the most tolerant fuel cell type to H_2S impurities (Hofmann et al., 2009), fuel cleaning should be included to remove H_2S.

One of the most promising technologies for removing H_2S to sub-ppm levels is adsorption on metal oxides. An adsorption media, typically zinc, copper, or iron oxide, is coated on a supporting material (Cherosky and Li, 2013). It is reported that the use of a Na–X zeolites fixed bed reactor and zinc oxide guard bed decreased the H_2S content from simulated biogas contaminated with traces of 30 ppm H_2S to 0.07 ppm (Papurello et al., 2014). Additionally, synthesised adsorbent materials like activated carbon are commonly used for H_2S removal in dry conditions and ambient temperature (Isik-Gulsac, 2016).

1.6. Research objective

To improve the sustainability of drinking water production from CH_4-containing anaerobic groundwater, we propose to use the recovered CH_4-rich gas as a fuel for SOFC and thereby reduce the carbon footprint. However, to our best knowledge, it remains unknown whether CH_4-rich gas from groundwater can be effectively used as fuel in an SOFC. To this end, CH_4-rich gas from a full-scale DWTP was sampled and, analysed and contaminants were removed. Finally, the cleaned CH_4-rich gas was fed to an SOFC to assess the feasibility of energy generation under both dry reforming and steam reforming conditions.

2. Materials and methods

2.1. CH_4 recovered from groundwater during drinking water production

A full-scale DWTP owned by Vitens N.V. produces drinking water from groundwater and has a maximum capacity of 25 million m3·year-1. The concentration of CH_4 in the groundwater ranges between 35 and 45 mg·L-1. The groundwater is pumped from the deep-wells directly to a system of vacuum towers, which remove 90 percent of the dissolved CH_4 using a vacuum depth of 0.2 bar(a). This results in a gas stream with a CH_4 concentration of 65–72 vol%. Subsequent treatment by plate aeration allows for the removal of the remaining 10 percent. Because plate aeration increases the concentration of O_2 in the water, iron is oxidised and iron hydroxide ($Fe(OH)_3$) flocs are formed, which are subsequently removed by media (sand and anthracite) filtration. After the media filtration, tower aeration is used to further remove CO_2 before pellet softening to lower hardness. Finally, any residual suspended solids are removed by another step of media filtration, and color is removed by anion exchange to produce a final water quality suitable as drinking water. The recovered CH_4-rich gas is currently utilised in a 550 kW (nominal power) gas turbine, which has an electrical efficiency in the order of 35%.

2.2. Recovered gas sampling

The CH_4-rich gas produced by the vacuum towers was sampled to conduct the experimental study by this recovered gas in the fuel cell lab. At this DWTP, water vapor in the recovered gas stream is condensed by cooling before the CH_4-rich gas storage. The CH_4-rich was sampled in three bags with a volume of 20 L (each) after the water vapor condensation. The sample bags were filled by connecting the bag to the recovered gas pipeline with a pressure of 22 mbar. The presence of H_2S in the CH_4-rich gas was measured directly after sampling, using a Dräger-Tube. Precipitation reactions of metal salts are the basis of measurement in the Dräger-Tube. Metal salts react with H2S and form soluble metal sulphides, which have a different color, and the contaminant level is visible through the shell of the Dräger-Tube. Additionally, the CH_4-rich gas was analysed in an Agilent 490 micro gas chromatograph, containing Molsieve 5A and PoraPLOT U columns. 200 mL of the CH_4-rich gas was used to determine the concentration of CH_4, H_2, O_2, nitrogen (N_2), CO, and CO_2.

2.3. Experimental SOFC set-up

A single cell SOFC test station (Fig. 1) was used to conduct the experiments. A planar nickel-coated scandium oxide stabilised zirconia (Ni-ScSZ) electrolyte supported cell (purchased from the Ningbo SOFCMAN Energy Technology Co., Ltd) with an effective surface area of 3.8 cm^2 was used for the experiments. The cell was placed between two Crofer metal plates, and gas tightness was achieved by sealing the cell with mica (thermiculite) sheets. Nickel foam and a gold mesh were used as current collectors at the anode and cathode, respectively. The cell and associated sealing were placed in a furnace to allow for a stable operational temperature.

The supply of synthetic N_2, O_2 and H_2 gas (with purity > 99.99%) was controlled by calibrated mass flow controllers (Bronkhorst High-Tech BV). The CH_4-rich gas was pumped from the sample bags to the anode by a suction pump (Hyco Vakuumtechnik GmbH), and the fuel flow rate was regulated by a calibrated rotameter. The fuel was initially pumped through a 500 mL gas reactor containing 225 g of impregnated steam activated extruded carbon (Norit® RGM 3) designed to remove low concentrations of sulfur compounds. A sampling point for the fuel was placed after the adsorption media reactor to determine the concentration of H_2S in the fuel after the pre-treatment (Fig. 1).

To allow for steam reforming of CH_4, demineralised water was injected into the fuel inlet by a calibrated peristaltic pump, having a flow rate range of 0.006–2300 $mL \cdot min^{-1}$ (Leadfluid Technology Co.). Due to the high temperature of the furnace and the low flow rate (ranging 1.8–9.2 $mL \cdot min^{-1}$) of the water, the water evaporated before reaching the anode. To validate that the supplied gases and steam affected the actual cell temperature, a k-type thermocouple was placed at the anode surface of the cell. The anode off-gas was connected to exhaust tubing, while the cathode off-gas was vented to the air.

Finally, electric measurements were performed by an electrochemical impedance spectroscopy (EIS) device (Gammry FC-350) by simultaneously measuring the electric potential while a variable resistance was set to draw the electric current.

After mounting the cell, the furnace was heated up to 850 °C with a ramp of 150 °C per hour. During the furnace heating, N_2 was fed to the anode and cathode at a flow rate of 200 $Nml \cdot min^{-1}$.

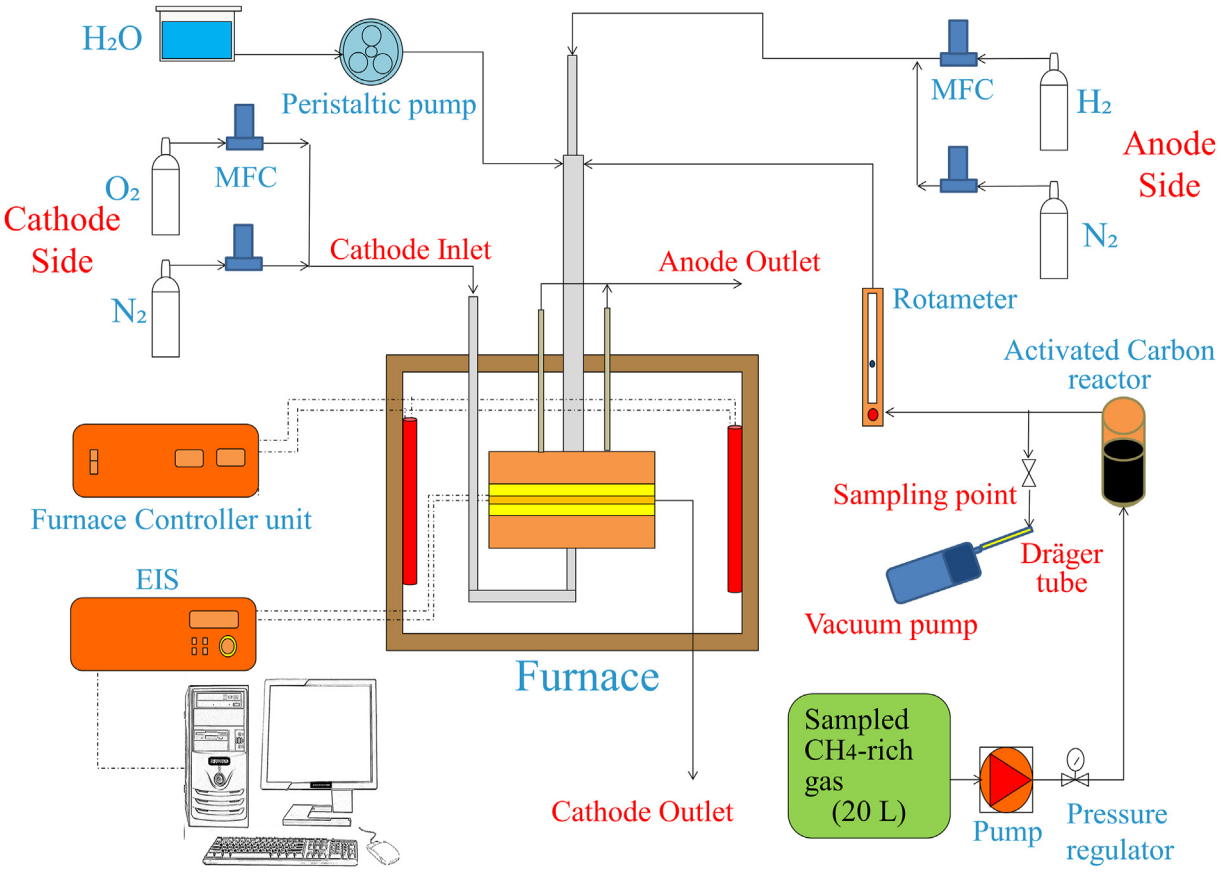

Fig. 1. A schematic representation of the experimental SOFC set-up.

Before using the CH_4-rich gas as fuel, the nickel catalyst was reduced because the nickel was initially present as nickel oxide (NiO) on the anode of the cell. The reduction of NiO, and thus the activation of the nickel catalyst, was achieved by feeding hydrogen to the anode at 850 °C. The H_2 flow rate was gradually increased to 200 Nml·min^{-1} while simultaneously, the N_2 flow rate was decreased from 200 to 0 Nml.min^{-1}. Throughout the entire operation of the SOFC air simulated by a controlled mixture of N_2 and O_2 was fed to the cathode at a flow rate of 400 and 110 NmL·min^{-1}, respectively. Subsequently, the cell temperature was decreased to 800 °C. A mixture of H_2 and N_2 was fed to the anode as a reference for the cell performance, at a flow rate of 140 and 60 NmL·min^{-1}, respectively. Subsequently, the CH_4-rich gas was fed to the anode at a flow rate of 200 NmL·min^{-1}, both solely and in combination with steam. After stabilising the electric potential during the feeding of the fuel, the open circuit potential (OCP) was logged. Finally, the electric circuit was closed, and the electric current was drawn stepwise (5 mA.s^{-1}), while logging the electric potential.

2.4. Thermodynamic approach

CH_4 must be reformed to H_2 and CO before electricity can effectively be generated in an SOFC. However, the deposition of carbon must be avoided, of which the risk is determined by the fuel gas composition and operating temperature at atmospheric pressure. FactSage thermochemical simulation software is used to determine the required amount of steam to prevent carbon deposition. FactSage software is mainly based on chemical equilibrium conditions by minimising Gibbs free energy. Carbon-based fuels typically consist of three key elements that are involved in carbon deposition: carbon (C), hydrogen (H) and oxygen (O). Ternary C–H–O phase diagrams are used to identify solid carbon formation regions based on the operating temperature, and the amount of required reforming agent (in this case, steam) can be determined to shift the operating condition with the gas composition to the safe operating region. However, the chemical equilibrium condition cannot be completely achieved.

Several studies have reported significant deviations between the equilibrium calculations and experimental measurements (Haseli, 2019). The deviation might vary based on the anode catalyst types and the size of nickel crystallites (Rostrup-Nielsen, 1972). Moreover, the fuel flow rate impacts the internal methane reforming in the SOFC due to the mass transfer effects at different fuel velocities (Laosiripojana and Assabumrungrat, 2005). The anode material also impacts the carbon deposition risk in hydrocarbon fuelled SOFCs. For instance, Takeguchi et al. (2002) claimed that the Ni–YSZ cermet structure is favourable for whisker carbon growth. The authors proposed a carbon growth formation mechanism based on the dissolution of adsorbed carbon atoms in the metal crystallite, diffusion of carbon atoms through the metal, and precipitation at the rear of the metal particle.

2.5. Performance indicators

To assess the feasibility of using the CH_4-rich gas as a fuel for an SOFC, both the open circuit potential and the power density at an electric potential of 0.6 V were determined. The theoretical open circuit (Nernst) potential is generally calculated based on H_2 or CO concentrations as reactants and H_2O or CO_2 as products of the electrochemical reactions (Penchini et al., 2013). However, in the

case of using both H_2 and CO gas in the fuel, the Nernst potential cannot be determined the conventional way (with H_2 partial pressure), as also the water gas shift reaction (WGSR, Eq. (3)) can take place (Ni, 2012). Therefore, the Nernst potential was calculated based on the concentration of O_2 at anode and cathode sides, according to the method of Leone et al. (2010) (Eq. (4)).

$$E_{TOC} = \frac{R \cdot T}{n \cdot F} \cdot \ln\left(\frac{p_{O_2,cathode}}{p_{O_2,anode}}\right) \quad (4)$$

Where R = universal gas constant (8.31 J mol·K^{-1}), T = operational temperature (in K), n = number of electrons transferred for each mole of O_2 (unitless, n = 4), F = Faraday constant (96,485 C·mol^{-1}) and P = partial pressure (in bar, $PO_{2,\ cathode}$ = 0.21 bar in atmospheric air).

The concentration of O_2 at the anode depends on the actual gas composition at the anode after reforming and must be calculated based on equilibrium condition (by FactSage software). The measured OCP was compared to the Nernst potential (Eq. (4)) to assess the efficiency of the CH_4 reforming. Besides the Nernst potential, the power density characterisation is also typically used to evaluate the SOFC performance with different fuels at different operating conditions (Saadabadi et al. (2019)). The peak power density is indicating electrical energy generated from the fuel per unit of SOFC surface.

Finally, the CH_4 conversion in the SOFC is calculated based on the carbon balance at the inlet and outlet at equilibrium condition. Based on the dry reforming reaction, 1 mol of CH_4 produces 2 mol of CO and can be calculated based on the outlet gas composition, as shown in Eq. (5) (Li et al., 2017).

$$X_{CH_4} = \frac{\gamma_{CH_4,in} - \gamma_{CH_4,out}}{\gamma_{CH_4,in}} \times 100(\%) = \frac{0.5 \cdot \gamma_{CO,out}}{\gamma_{CH_4,out} + 0.5 \cdot \gamma_{CO,out}} \times 100(\%) \quad \text{Eq. 5}$$

Where X_{CH4} = CH_4 reforming (%), γ_i is the mole fraction of gas species 'i' in the inlet and outlet of the SOFC (unitless). It is essential to mention that the CH_4 conversion is calculated based on the gas concentration in the gas phase, and the carbon deposition is neglected.

3. Results and discussion

3.1. Composition and pre-treatment of CH_4-rich gas

The concentration of CH_4 in the gas recovered from the DWTP was 71.4 mol. % (with standard deviation σ = 1.83 and number of samples of r = 8). In addition to CH_4, the recovered gas contained 23 mol% CO_2 and 5 mol% N_2 and a trace of oxygen and H_2S (average of 9 ppm). The composition of the gas is similar to biogas generated during the anaerobic digestion, which also mainly contains CH_4 and CO_2 in the range of 70–45 and 60 - 40%, respectively (Jahn et al., 2013).

The measurement of H_2S in the recovered gas after the pre-treatment indicates that the use of activated carbon as adsorbent was sufficient to decrease the content of H_2S from 9 to below 0.1 ppm, which is an acceptable level for SOFC applications (Papadias et al., 2012). The residence time of the gas of 150 s allowed for sufficient contact time to adsorb the H_2S. Because the content of H_2S was already below the detection limit, the effectivity of the other adsorbents was not further considered.

3.2. Reforming procedure of the CH_4-rich gas

Because the CH_4-rich gas contains a lower fraction of CO_2 compared to CH_4, dry reforming could lead to carbon formation, and thus the addition of steam is required to reform the CH_4. Adding steam to the CH_4-rich gas fuel leads to a decrease in the concentration of CH_4 at OCP operating condition, as presented in Fig. 2A. As explained in 2.3, carbon deposition can be predicted by FactSage.

Fig. 2B presents the gas concentrations at equilibrium conditions (at 800 °C) after reforming the CH_4-rich gas mixed with steam (S/C ratio up to 1). When the recovered CH_4 is reformed without steam (S/C ratio = 0), carbon deposition takes place, and there is still 2.3 mol% CH_4 present, which is not reformed to H_2 and CO. Meanwhile, the CO_2 concentration decreases to 0.7 mol% due to the dry reforming reaction. By adding steam to the CH_4-rich gas, methane-steam reforming also takes place, and the equilibrium CH_4 concentration decreases to 1.3 mol%, and only 3.5 mol% of steam remains at an S/C of 0.6. Moreover, CO_2 in biogas also contributes to the methane dry reforming reaction and WGSR (Jiang and Virkar, 2003), resulting in a decrease of the CO_2 concentration to less than 2 mol%. Due to the higher concentration of steam at the S/C ratio of 1.0, the steam and CO_2 concentrations in the reformed gas (at equilibrium) increase to 11 and 4.6 mol.%, respectively.

The carbon deposition threshold for different operating temperatures of SOFCs is visualised in the C–H–O ternary diagram in Fig. 3. The gas composition of the CH_4-rich gas is located in the carbon deposition region. Adding steam as a reforming agent moves the operating condition into the safe region by increasing the concentration of H and O elements in the fuel. A steam to carbon (S/C) ratio of 0.6 is required for the safe operation of SOFC at 800 °C. However, local temperature drops due to the endothermic reforming reactions, can still lead to local carbon deposition. Increasing the S/C ratio to 1.0 brings the operating condition to the safe region even at lower cell temperatures (around 700 °C). However, the long-term safe operation should be experimentally investigated for different operating conditions.

Furthermore, increasing the steam concentration of the fuel increases the CH_4 reforming rate, as presented in Fig. 4. At equilibrium conditions at 800 °C, the CH_4 conversion increases from 82% (through the dry reforming reaction) to around 98% when instead of only dry reforming, also steam reforming takes place due to the addition of steam. By increasing the S/C ratio to 0.6, carbon deposition is suppressed at equilibrium condition, and this leads to a sudden increase in the CH_4 conversion rate, as shown in Fig. 4. The concentration of formed solid carbon (graphite) with various S/C ratios at equilibrium conditions is presented in Fig. 4.

However, the increasing contribution of steam reforming in comparison to dry reforming does not necessarily lead to an increase in H_2 concentration (according to the H_2/CO ratios of Eq. 1 and 2). Increasing steam concentration to S/C of 1.0 increases the concentration of unreacted steam in the reformed gas composition, and this decreases the H_2 and CO concentrations. Moreover, increasing the H_2 concentration shifts the WGSR equilibrium (Eq. 3) toward the reactants (CO and H_2O), which again leads to a decrease in H_2 concentration. Ultimately, the results of equilibrium calculations (Fig. 2B) show that increasing the conversion of CH_4 by increasing the steam concentration does not lead to a higher concentration of H_2 and CO.

Fig. 5 presents the Nernst potential for different gas compositions with the S/C ratio ranging between 0 and 1.0, calculated using Eq. (4). When the S/C < 0.6, by increasing S/C, the H_2 concentration decreases. In contrast, the CO concentration increases. Thus, the Nernst voltage does not significantly change. When the S/C ≥ 0.6,

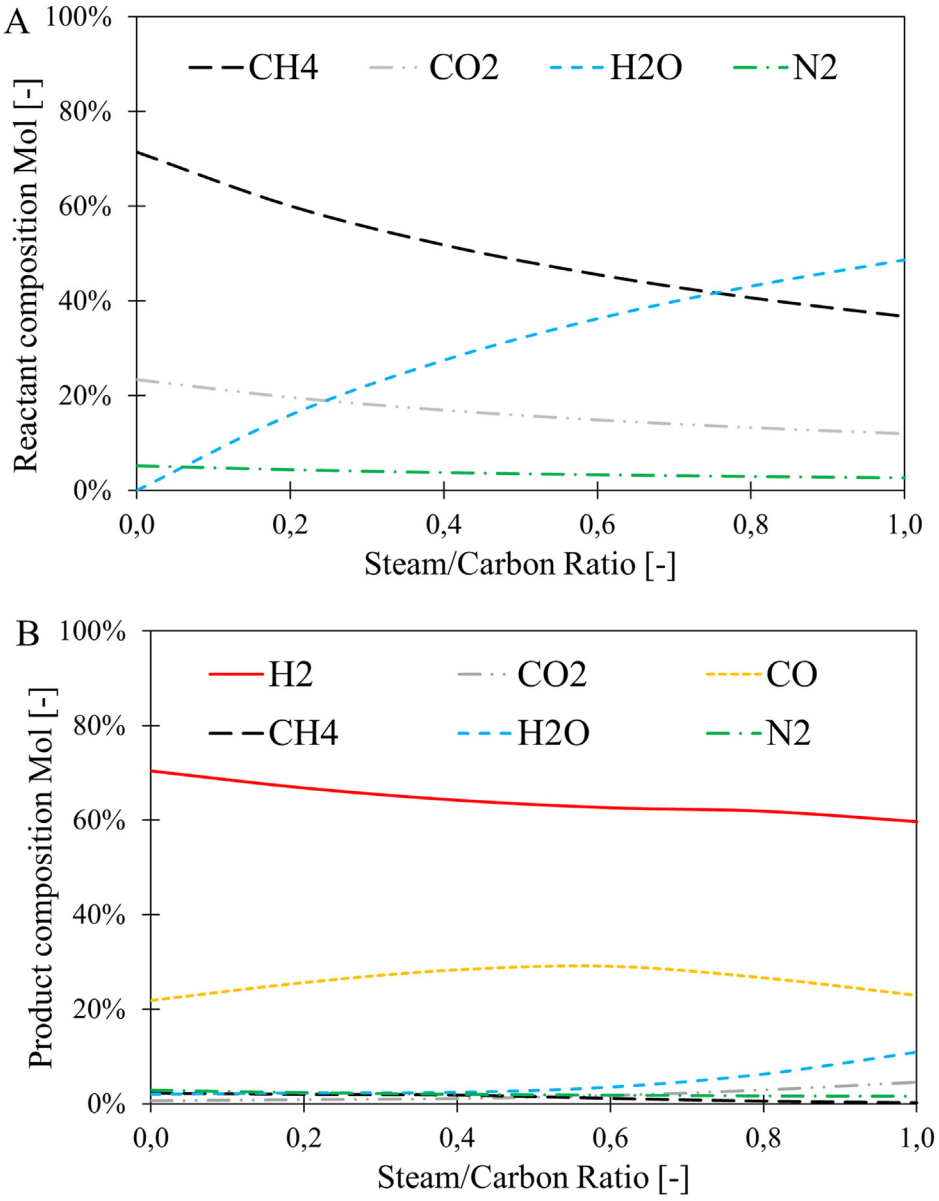

Fig. 2. The gas composition of fuel at the inlet of SOFC before reforming (A). Increasing the S/C ratio by adding more steam results in the dilution of CH_4, CO_2 and N_2 and increased presence of H_2O in the fuel mixture. The gas composition of reformed fuel, according to equilibrium condition at 800 °C (B). Increasing the S/C ratio to 0.6 leads to an increase in the presence of CO, while the presence of H_2 decreases. By further increasing the S/C ratio to 1.0, H_2 and CO are further diluted, but the risk of local carbon deposition is decreased.

due to remaining steam and CO_2 in the reformed gas, both H_2 and CO concentrations decrease. Therefore, the Nernst voltage drops by increasing the S/C. However, despite the lower Nernst potential, increasing the S/C ratio is necessary to prevent carbon deposition.

3.3. Performance of the solid oxide fuel cell on CH_4-rich gas

After the reduction of NiO to nickel, the cell performance was tested at 800 °C. A mixture of H2 (100 NmL·min^{-1}) and N2 (60 NmL·min^{-1}) was used as a reference for the performance of the cell. The electric potential measurements and I–V characterisation were performed after the stabilisation of temperature and electric potential. The measured OCP with H_2 and N_2 was 1.21 V, which corresponded well with the Nernst potential at 800 °C (1.24 V), implying that there was negligible H_2 leakage inside the setup (Li et al., 2019). Fig. 6 presents the I–V characterisation and shows that the electric potential gradually decreased to 0.65 V, at a rate of 5 mA.s^{-1} until an electric current density of 155 mA·cm^{-2} was achieved. Subsequently, the CH_4-rich gas was fed to the cell, while the flow rate of H_2 was gradually decreased to 0 mL·min^{-1}. The measured OCP was 1.11 V when solely the CH_4-rich gas was fed to the cell, which again corresponded well with the Nernst potential at equilibrium conditions (1.10 V), indicating that the concentrations of H_2 and CO are similar to the equilibrium calculations, and the same (internal dry) CH_4 reforming is achieved. After stabilisation of the electric potential, the I–V characterisation was conducted. By increasing the electric current density, the electric potential dropped to 0.6 V at 150 mA·cm^{-2}. The ohmic cell resistance (the slope of the curve at high electric current densities) is the same for H_2 and the CH_4-rich gas, as can be seen in Fig. 6.

According to the equilibrium calculations, operating an SOFC with the CH_4-rich gas composition (CH4 concentration of 70 mol%) results in carbon deposition in long-term operation, which was experimentally investigated by Lanzini and Leone (2010). The OCP

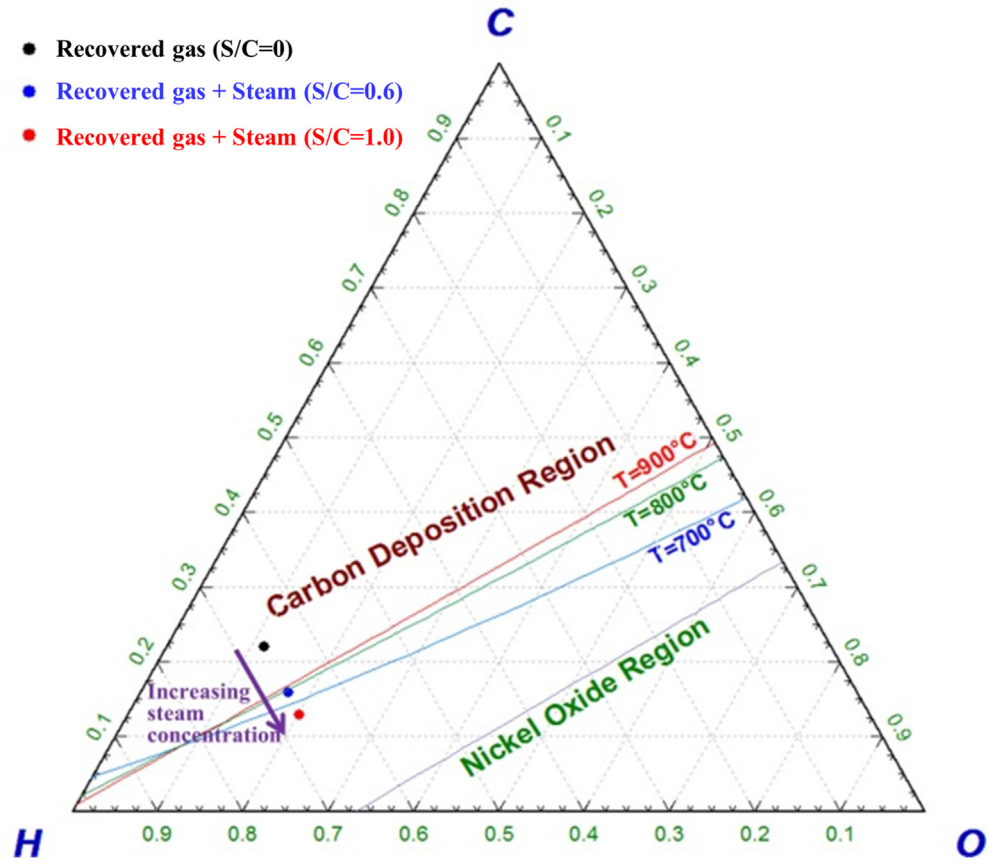

Fig. 3. The C–H–O ternary diagram indicating solid carbon formation (based on equilibrium calculations) for various S/C ratios and operating temperatures at atmospheric pressure.

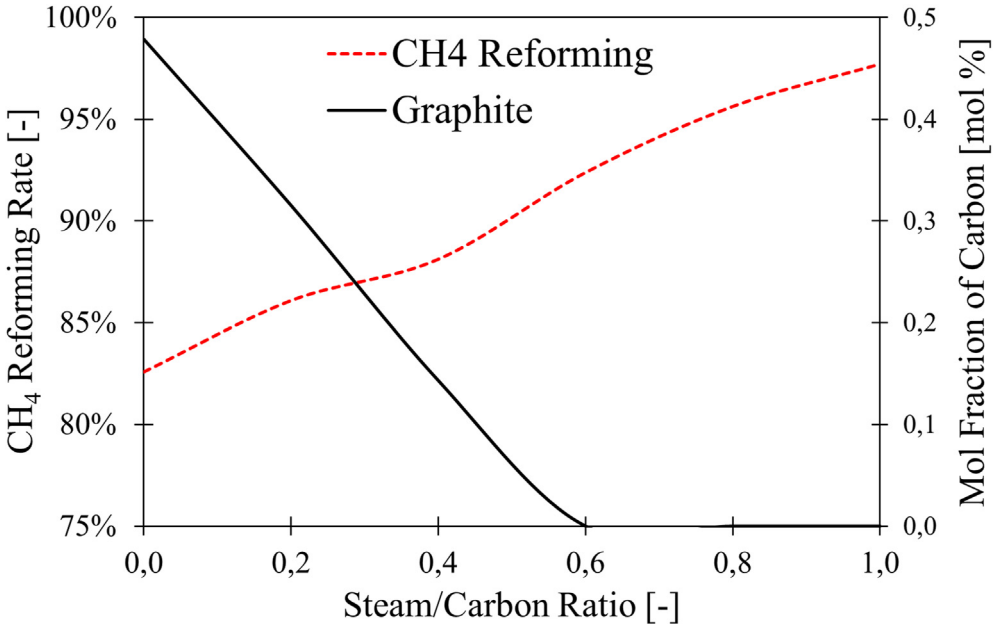

Fig. 4. When the S/C ratio increases, the reforming of CH_4 increases, while simultaneously the amount of carbon deposition (graphite formation) decreases, according to equilibrium calculations. At an S/C ratio of 0.6, no carbon deposition is expected.

decreased from 1.11 V (for dry reforming conditions) to 1.02 V (for steam reforming conditions) by adding steam to allow for steam reforming. The measured OCP was equal to the Nernst potential (1.02 V), again indicating that CH_4 was almost completely reformed to H_2 and CO. Similar results regarding the high CH_4 reforming with the S/C ratio of 0–3 has been observed in the study of Timmermann

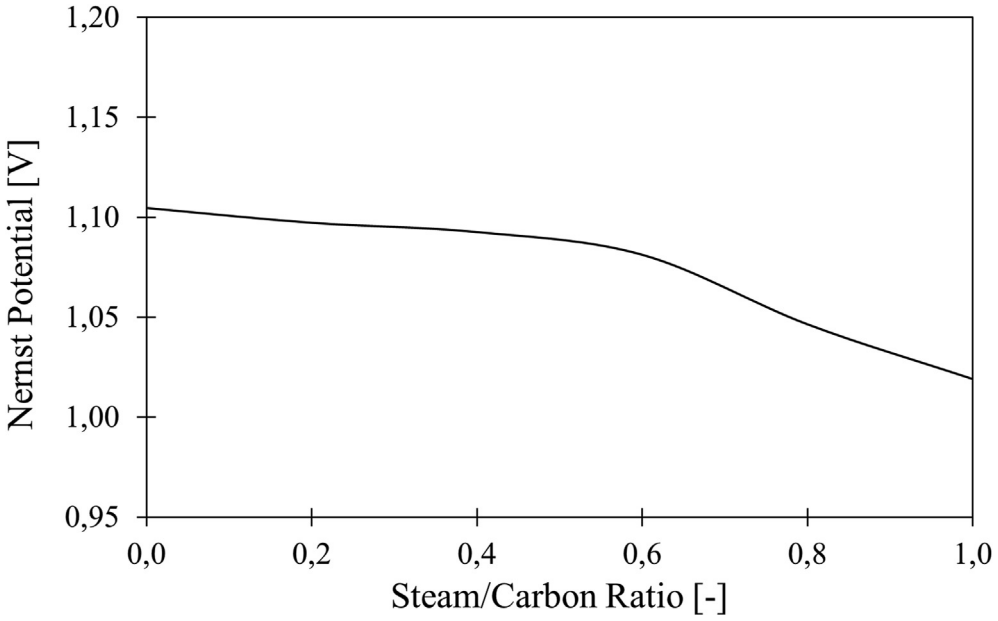

Fig. 5. The calculated Nernst potential decreases when the S/C ratio increases, because the partial pressure of H_2 and CO decrease due to dilution, and the partial pressure of water increases due to the addition of steam.

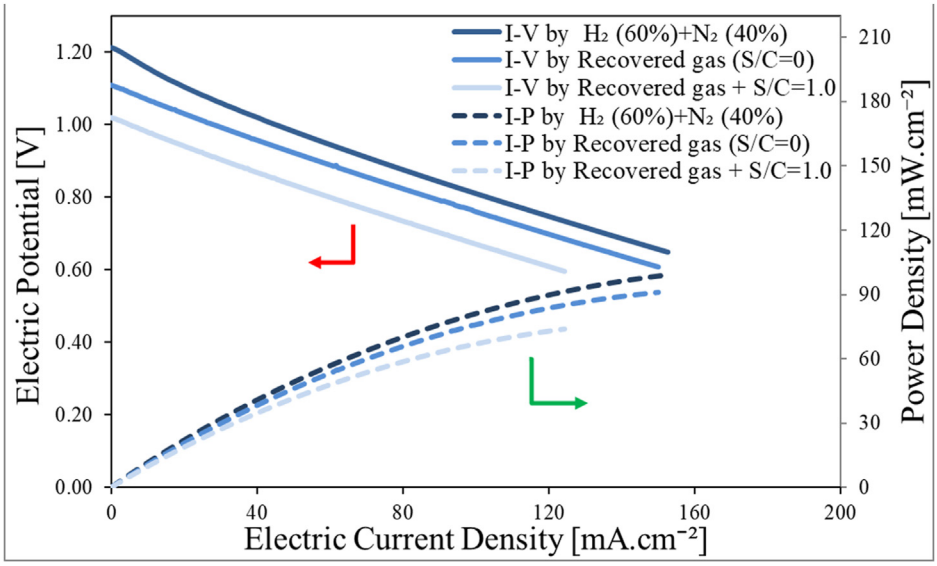

Fig. 6. The I–V characterisation of the cell and the determination of the peak power density for the various tested fuel compositions. The OCPs agreed well with the calculated Nernst potentials of the various fuels. The maximum current and power density of the CH_4-rich gas for steam reforming conditions (required to avoid carbon deposition) were lower than for dry reforming conditions because the OCP was lower due to steam added.

et al. (2006). However, an electric potential fluctuation (±2 mV) was observed, caused by the non-uniform fuel-steam gas mixture. The I–V characterisation of the cell performance with CH_4-rich gas and steam reforming is presented in Fig. 6. As a result of the lower OCP, the maximum achieved current density at 0.6 V was 123 mA·cm^{-2}, which is lower than the achieved current density with H_2 and the CH_4-rich gas at dry reforming conditions. Due to higher ohmic resistance of electrolyte supported cells, the obtained current densities in this study are lower than the CH_4 fed SOFC with anode supported (Ni-YSZ) cells with the current densities in a range of 500 mA·cm^{-2} (Leone et al., 2010). However, the cell resistance in this study is lower than the test carried out by Goula et al. (2006), who used a button Ni-YSZ cell at dry reforming condition and achieved a current density of 95 mA·cm^{-2}. The cell resistance in this study is comparable with the results reported by Timmermann et al. (2006), who reported a current density of 140 mA·cm^{-2} using an S/C ratio of 1.0 with both Ni-YSZ and Ni-GDC anodes, electrolyte supported cell. However, the cell resistance in this study is higher than a test with commercialized electrolyte supported Ni-YSZ cell, achieving a current density of 300 mA·cm^{-2} (Lanzini and Leone, 2010). Hence, the cell performance in this study might be improved further by selecting a proper cell material for this operating condition (Saadabadi et al., 2019).

The power density curves for the different fuels are calculated (based on the I–V characterisation) and presented in Fig. 6. Due to a lower OCP, the maximum power generation while using the CH4-

rich gas with steam reforming (72 $mW \cdot cm^{-2}$) was lower than for using H2 (99 $mW \cdot cm^{-2}$) and CH_4-rich (89 $mW \cdot cm^{-2}$) at dry reforming conditions. Achieving a lower power density implies that a larger SOFC stack should be used for the CH_4-rich gas fuelled SOFC system with steam reforming, compared to dry reforming. However, the use of steam reforming avoids any risk of carbon deposition, according to the experimental results of Lanzini and Leone (2010).

3.4. Power generation and CO_2 emission

The previous section showed that the CH_4 recovered from groundwater could be effectively used as fuel in an SOFC stack. The implications for the electrical power generation and the reduction of the carbon footprint by applying an SOFC system at the considered DWTP are discussed in this section. Considering a CH_4 removal efficiency of 90% and a hydraulic flow rate of 3.2×10^3 $m^3 \cdot h^{-1}$ in this DWTP, the CH_4 production is 8.08×10^3 $mol \cdot hr^{-1}$.

Based on the equilibrium calculations (by FactSage), steam reforming of CH_4 with an S/C ratio of 1.0, 2.82 mol of H_2, and 1.11 mol of CO can be produced from each mole of CH_4. The Gibbs free energy of the reformed CH_4 at 800 °C is −742 $kJ \cdot mol^{-1}$. With an assumption of the SOFC electrical efficiency of 55% at fuel utilisation of 85% (Gandiglio et al., 2014), the electrical power generation of the SOFC system at this DWTP can be 915 kW. Hence, this SOFC system can supply 51.2% of the electrical power demands of the entire DWTP, which is 365 kW more than the power generated in the current gas engine system. We must emphasise that the heat demands of CH_4 reforming also can be supplied by heat generated in the SOFC stack (Saadabadi et al., 2019).

The high efficiency of SOFC systems can help in reducing the carbon footprint of the DWTP. The annual power generation of the SOFC system can be 8015 MWh, which is 3197 MWh more than produced by the gas engine installation. The CO_2 emission of natural gas-fuelled power plants in Europe is approximately 561 g-$CO_2 \cdot kWh^{-1}$ (Wang and Sun, 2012). Therefore, developing a 915 kW SOFC system at the Spannenburg plant can reduce the carbon footprint of the plant by 1794 tons CO_2 per year. Furthermore, the recovered gas utilisation in the SOFC system extremely reduces the NOx emissions (Krist et al., 1999). The energetic and carbon emission implications are summarised in Table 1.

3.5. Future outlook

In this study, the performance of a single cell SOFC fuelled with CH_4 recovered from groundwater was investigated. To further develop an SOFC system fuelled with CH_4-rich gas, additional studies on different levels are required. First of all, a long-term durability test should be conducted to identify the optimum fuel processing conditions, including CH_4 reforming and H_2S cleaning, to determine the carbon deposition threshold at different operating conditions such as temperature, current density, and especially the fuel utilisation.

A long-term test is encouraged to identify the H_2S adsorption capacity of activated carbon for the recovered gas at the operating condition. Moreover, the sustainability of the DWTP can be improved by considering the iron oxide (by-product of this DWTP) material for the H_2S removal in the gas cleaning unit.

The focus of this study was to investigate the possibility of using CH_4-rich gas as fuel. However, the fuel utilisation was in the range of a few percentages due to the limitation of the capacity of the gas flow controller, while the fuel utilisation can reach 85% in the SOFC stack. By using an anode supported cell instead of the electrolyte supported cell (in this study), the performance of the SOFC system can potentially be improved by enhancing the internal CH_4 reforming (due to the higher catalytic surface area) and decreasing the ohmic resistance of the cell (Lanzini and Leone, 2010). After identifying an optimised fuel processing and selecting a proper cell material for the operating condition, a long-term test should be conducted to determine the safe operating condition with respect to the carbon deposition issue. These tests should be extended to the SOFC stack level and pilot plant (in the range of a few kW systems).

Moreover, the sustainability of the considered DWTP can be further improved by heat integration of the SOFC system (Trendewicz and Braun, 2013). Generated heat in the SOFC stack can be utilised in sub-processes of the treatment plant. Furthermore, because of the high concentration of CO_2 in the exhaust of the SOFC system, there is an opportunity to capture CO_2 and recycle it in the CH_4 removal or pellet softening process of the DWTP (Campanari et al., 2016). Eventually, a specific SOFC system can be designed and developed for the DWTPs based on the lessons learned from such studies.

4. Conclusions

High concentrations of CH_4 in groundwater used for the production of drinking water cause sustainability issues at DWTPs concerning greenhouse gas emissions. Technologies such as vacuum stripping allow for the recovery of CH_4 from groundwater and the subsequent use of the CH_4-rich gas as a fuel. We proposed to use SOFC as an efficient energy-conversion technology to improve the sustainability of DWTPs and assessed the feasibility of using CH_4-rich gas extracted from the water of a full-scale DWTP, a proof of principle test in this study.

Recovered gas from the DWTP in Spannenburg (the Netherlands) was collected and analysed. The main components in the sampled gas were CH_4 and CO_2 with concentrations of 71 and

Table 1
The projected power generation and carbon footprint of the DWTP of Vitens concerning the current gas engine system and the potential SOFC system.

	Unit	Gas engine system	SOFC system
Recovery CH_4 Utilisation at DWTP			
System power	kW	550	915
System efficiency	–	35% (Trendewicz and Braun, 2013)	55% (Gandiglio et al., 2014)
Percentage of power demand	–	30.8%	51.2%
Power supplied by the grid	kW	1238	873
Energetic advantage	–	20.4%	
Annual CO_2 Emissions			
Local CO_2 emissions: from power system	ton-CO_2	4136	4136
CO_2 emissions: CH_4 Utilisation at DWTP	g-$CO_2 \cdot kWh^{-1}$	858	516
CO_2 emissions: Power from grid (Wang and Sun, 2012)	ton-CO_2	6084	4290
Total CO_2 emission of the DWTP	ton-CO_2	10,220	8426
CO_2 emission advantage	–	−17.6%	

23 mol%, respectively. Additionally, the recovered gas contained 9 ppm of H_2S, which can permanently influence the cell performance of the SOFC. H_2S was effectively removed (<0.1 ppm) with impregnated activated carbon with a residence time of 150 s at ambient temperature.

Thermodynamic calculations based on equilibrium conditions showed that using CH_4 directly in SOFCs results in carbon deposition and deactivation of the anode in long-term operation. The content of CO_2 in the recovered gas was not sufficient to allow for complete dry reforming of CH_4. Therefore, extra steam should be added to the CH_4-rich gas to increase the CH_4 conversion by steam reforming. An S/C ratio of 0.6 was the minimum required value to prevent carbon deposition at an operating temperature of 800 °C. However, endothermic reforming reactions at the anode fuel channel cause local temperature gradients, which increase the risk of local carbon deposition. Therefore, the cell performance was experimentally determined at an S/C ratio of 1.0. The OCP was in line with the calculated Nernst potential, indicating a high CH_4 reforming rate. A peak power density of 72 $mW \cdot cm^{-2}$ was achieved with the CH_4-rich gas at an S/C ratio of 1.0. Further experimental studies concerning optimisation of the operating conditions and cell and stack design are required to develop an efficient SOFC system suitable for using CH_4-rich gas in DWTPs.

The use of CH_4 recovered from the groundwater in an SOFC opens up opportunities to mitigate the greenhouse gas emissions and improve the sustainability of DWTPs. The recovered CH_4 of the Spannenburg DWTP can be used to run a 915 kW SOFC system. This can supply 51.2% of the total electrical power demand of the plant and decreases greenhouse gas emissions by 17.6%, which is around 1794 tons of CO_2.

Ongoing and future works: Currently, a larger SOFC (a few kW) system has been integrated at the DWTP Spannenburg, the Netherlands. The tests with the actual recovered CH_4-rich gas are being conducted. The results are beyond the scope of this paper. Analyzing and reporting the results will be considered as a follow-up publication.

CRediT authorship contribution statement

S. Ali Saadabadi: Conceptualization, Methodology, Formal analysis, Investigation, Resources, Data curation, Writing - original draft, Visualization, Project administration. **Niels van Linden:** Conceptualization, Methodology, Formal analysis, Writing - review & editing. **Abel Heinsbroek:** Conceptualization, Resources, Funding acquisition. **P.V. Aravind:** Validation, Supervision.

Declaration of competing interest

The authors declare that they have no known competing financial interests or personal relationships that could have appeared to influence the work reported in this paper.

Nomenclature

AVG	Average
CH_4	Methane
CO	Carbon monoxide
CO_2	Carbon dioxide
DWTP	Drinking water treatment plant
E	Electric potential (V)
EIS	Electrochemical Impedance Spectroscopy
F	Faraday constant in ($C \cdot mol^{-1}$)
H_2	Hydrogen
H_2S	Hydrogen sulphide
MFC	Mass flow controller
mA	Milli amps
N_2	Nitrogen
n	Number of electrons
Ni	Nickel
NiO	Nickel oxide
NmL	Normal millilitre (at 0 °C and P = 1 bar)
O_2	Oxygen
OCP	Open circuit potential
P	Partial pressure (bar)
ppm	Parts per million
r	Number of samples
R	Universal gas constant ($J \cdot mol \cdot K^{-1}$)
S/C	Steam to carbon ratio
ScSZ	Scandium oxide stabilised zirconia
SOFC	Solid oxide fuel cell
T	Operational temperature (K)
X	Conversion rate

Greek Symbols

σ	Standard deviation
γ	Mole fraction
ΔH^0	Enthalpy change ($kJ.mol^{-1}$)

Subscripts

e	Electric power
i	Gas species
in	Inlet
out	Outlet
TOC	Theoretical open circuit

References

Abatzoglou, N., Boivin, S., 2009. A review of biogas purification processes. Biofuels Bioprod. Biorefin. 3 (1), 42–71.

Ahmad, A., van der Wens, P., Baken, K., de Waal, L., Bhattacharya, P., Stuyfzand, P., 2020. Arsenic reduction to <1 μg/L in Dutch drinking water. Environ. Int. 134, 105253.

Appari, S., Janardhanan, V.M., Bauri, R., Jayanti, S., 2014. Deactivation and regeneration of Ni catalyst during steam reforming of model biogas: an experimental investigation. Int. J. Hydrogen Energy 39 (1), 297–304.

Bao, J., Krishnan, G.N., Jayaweera, P., Lau, K.-H., Sanjurjo, A., 2009. Effect of various coal contaminants on the performance of solid oxide fuel cells: Part II. ppm and sub-ppm level testing. J. Power Sources 193 (2), 617–624.

Campanari, S., Mastropasqua, L., Gazzani, M., Chiesa, P., Romano, M.C., 2016. Predicting the ultimate potential of natural gas SOFC power cycles with CO2 capture–Part B: Applications. J. Power Sources 325, 194–208.

Chen, T., Wang, W.G., Miao, H., Li, T., Xu, C., 2011. Evaluation of carbon deposition behavior on the nickel/yttrium-stabilized zirconia anode-supported fuel cell fueled with simulated syngas. J. Power Sources 196 (5), 2461–2468.

Cherosky, P., Li, Y., 2013. Hydrogen sulfide removal from biogas by bio-based iron sponge. Biosyst. Eng. 114 (1), 55–59.

EurEau, 2019. Reducing the Energy Footprint of the Water Sector. EurEau, Brussels.

Fan, L., van Biert, L., Thallam Thattai, A., Verkooijen, A.H.M., Aravind, P.V., 2015. Study of methane steam reforming kinetics in operating solid oxide fuel cells: influence of current density. Int. J. Hydrogen Energy 40 (15), 5150–5159.

Farhad, S., Hamdullahpur, F., Yoo, Y., 2010. Performance evaluation of different configurations of biogas-fuelled SOFC micro-CHP systems for residential applications. Int. J. Hydrogen Energy 35 (8), 3758–3768.

Gandiglio, M., Lanzini, A., Santarelli, M., Leone, P., 2014. Design and balance-of-plant of a demonstration plant with a solid oxide fuel cell fed by biogas from wastewater and exhaust carbon recycling for algae growth. J. Fuel Cell Sci. Technol. 11 (3), 031003.

Girona, K., Laurencin, J., Fouletier, J., Lefebvre-Joud, F., 2012. Carbon deposition in CH4/CO2 operated SOFC: simulation and experimentation studies. J. Power Sources 210, 381–391.

Goula, G., Kiousis, V., Nalbandian, L., Yentekakis, I.V., 2006. Catalytic and electrocatalytic behavior of Ni-based cermet anodes under internal dry reforming of CH4+CO2 mixtures in SOFCs. Solid State Ionics 177 (19), 2119–2123.

Gür, T.M., 2016. Comprehensive review of methane conversion in solid oxide fuel cells: prospects for efficient electricity generation from natural gas. Prog. Energy Combust. Sci. 54, 1–64.

Haseli, Y., 2019. Criteria for chemical equilibrium with application to methane steam reforming. Int. J. Hydrogen Energy 44 (12), 5766–5772.

Hofmann, P., Panopoulos, K.D., Aravind, P.V., Siedlecki, M., Schweiger, A., Karl, J., Ouweltjes, J.P., Kakaras, E., 2009. Operation of solid oxide fuel cell on biomass

product gas with tar levels >10 g Nm−3. Int. J. Hydrogen Energy 34 (22), 9203–9212.
Isik-Gulsac, I., 2016. Investigation of impregnated activated carbon properties used in hydrogen sulfide fine removal. Braz. J. Chem. Eng. 33 (4), 1021–1030.
Jahn, M., Heddrich, M., Weder, A., Reichelt, E., Lange, R., 2013. Oxidative dry-reforming of biogas: reactor design and SOFC system integration. Energy Technol. 1 (1), 48–58.
Jiang, Y., Virkar, A.V., 2003. Fuel composition and diluent effect on gas transport and performance of anode-supported SOFCs. J. Electrochem. Soc. 150 (7), A942–A951.
Krist, K., Gleason, K.J., Wright, J.D., 1999. SOFC-based residential cogeneration systems. ECS Proc. 1999 (1), 107.
Kulongoski, J.T., Mcmahon, P.B., 2019. Methane emissions from groundwater pumping in the USA. npj Clim. Atmos. Sci. 2 (1), 1–8.
Lanzini, A., Leone, P., 2010. Experimental investigation of direct internal reforming of biogas in solid oxide fuel cells. Int. J. Hydrogen Energy 35 (6), 2463–2476.
Laosiripojana, N., Assabumrungrat, S., 2005. Catalytic dry reforming of methane over high surface area ceria. Appl. Catal. B Environ. 60 (1–2), 107–116.
Lapworth, D.J., Baran, N., Stuart, M.E., Ward, R.S., 2012. Emerging organic contaminants in groundwater: a review of sources, fate and occurrence. Environ. Pollut. 163, 287–303.
Leone, P., Lanzini, A., Santarelli, M., Calì, M., Sagnelli, F., Boulanger, A., Scaletta, A., Zitella, P., 2010. Methane-free biogas for direct feeding of solid oxide fuel cells. J. Power Sources 195 (1), 239–248.
Li, M., Hua, B., Luo, J.-L., 2017. Alternative fuel cell technologies for cogenerating electrical power and syngas from greenhouse gases. ACS Energy Lett. 2 (8), 1789–1796.
Li, R., Liang, X., Wang, X., Zeng, W., Yang, J., Yan, D., Pu, J., Chi, B., Li, J., 2019. Improvement of sealing performance for Al2O3 fiber-reinforced compressive seals for intermediate temperature solid oxide fuel cell. Ceram. Int. 45 (17), 21953–21959. Part A.
Mahato, N., Banerjee, A., Gupta, A., Omar, S., Balani, K., 2015. Progress in material selection for solid oxide fuel cell technology: a review. Prog. Mater. Sci. 72, 141–337.
Mikalsen, R., Wang, Y.D., Roskilly, A.P., 2009. A comparison of Miller and Otto cycle natural gas engines for small scale CHP applications. Appl. Energy 86 (6), 922–927.
Ni, M., 2012. Modeling of SOFC running on partially pre-reformed gas mixture. Int. J. Hydrogen Energy 37 (2), 1731–1745.
Osborn, S.G., Vengosh, A., Warner, N.R., Jackson, R.B., 2011. Methane contamination of drinking water accompanying gas-well drilling and hydraulic fracturing. Proc. Natl. Acad. Sci. U. S. A 108 (20), 8172–8176.
Ouweltjes, J., Aravind, P., Woudstra, N., Rietveld, G., 2006. Biosyngas utilization in solid oxide fuel cells with Ni/ GDC anodes. J. Fuel Cell Sci. Technol. 3 (4), 495–498.
Papadias, D.D., Ahmed, S., Kumar, R., 2012. Fuel quality issues with biogas energy – an economic analysis for a stationary fuel cell system. Energy 44 (1), 257–277.
Papurello, D., Borchiellini, R., Bareschino, P., Chiodo, V., Freni, S., Lanzini, A., Pepe, F., Ortigoza, G.A., Santarelli, M., 2014. Performance of a solid oxide fuel cell short-stack with biogas feeding. Appl. Energy 125, 254–263.
Penchini, D., Cinti, G., Discepoli, G., Sisani, E., Desideri, U., 2013. Characterization of a 100 W SOFC stack fed by carbon monoxide rich fuels. Int. J. Hydrogen Energy 38 (1), 525–531.
Rongwong, W., Goh, K., Bae, T.-H., 2018. Energy analysis and optimization of hollow fiber membrane contactors for recovery of dissolve methane from anaerobic membrane bioreactor effluent. J. Membr. Sci. 554, 184–194.
Rostrup-Nielsen, J.R., 1972. Equilibria of decomposition reactions of carbon monoxide and methane over nickel catalysts. J. Catal. 27 (3), 343–356.
Saadabadi, S.A., Thallam Thattai, A., Fan, L., Lindeboom, R.E.F., Spanjers, H., Aravind, P.V., 2019. Solid oxide fuel cells fuelled with biogas: potential and constraints. Renew. Energy 134, 194–214.
Sasaki, K., Adachi, S., Haga, K., Uchikawa, M., Yamamoto, J., Iyoshi, A., Chou, J.-T., Shiratori, Y., Itoh, K., 2007. Fuel impurity tolerance of solid oxide fuel cells. ECS Trans. 7 (1), 1675–1683.
Sasaki, K., Haga, K., Yoshizumi, T., Minematsu, D., Yuki, E., Liu, R.-R., Uryu, C., Oshima, T., Taniguchi, S., Shiratori, Y., Ito, K., 2011. Impurity poisoning of SOFCs. ECS Trans. 35 (1), 2805–2814.
Stambouli, A.B., Traversa, E., 2002. Solid oxide fuel cells (SOFCs): a review of an environmentally clean and efficient source of energy. Renew. Sustain. Energy Rev. 6 (5), 433–455.
Staniforth, J., Ormerod, R.M., 2003. Running solid oxide fuel cells on biogas. Ionics 9 (5–6), 336–341.
Stocker, T.F., Qin, D., Plattner, G.-K., Tignor, M., Allen, S.K., Boschung, J., Nauels, A., Xia, Y., Bex, V., Midgley, P.M., 2013. Climate Change 2013: the Physical Science Basis. Contribution of Working Group I to the Fifth Assessment Report of the Intergovernmental Panel on Climate Change 1535.
Takeguchi, T., Kani, Y., Yano, T., Kikuchi, R., Eguchi, K., Tsujimoto, K., Uchida, Y., Ueno, A., Omoshiki, K., Aizawa, M., Takeguchi et al., 2002. Study on steam reforming of CH4 and C2 hydrocarbons and carbon deposition on Ni-YSZ cermets. J. Power Sources 112 (2), 588–595.
Timmermann, H., Fouquet, D., Weber, A., Ivers-Tiffée, E., Hennings, U., Reimert, R., 2006. Internal reforming of methane at Ni/YSZ and Ni/CGO SOFC cermet anodes. Fuel Cell. 6 (3-4), 307–313.
Tjaden, B., Gandiglio, M., Lanzini, A., Santarelli, M., Järvinen, M., 2014. Small-scale biogas-SOFC plant: technical analysis and assessment of different fuel reforming options. Energy Fuel. 28 (6), 4216–4232.
Trendewicz, A., Braun, R., 2013. Techno-economic analysis of solid oxide fuel cell-based combined heat and power systems for biogas utilization at wastewater treatment facilities. J. Power Sources 233, 380–393.
Velasco, P., Jegatheesan, V., Othman, M., 2018. Recovery of dissolved methane from anaerobic membrane bioreactor using degassing membrane contactors. Front. Environ. Sci. 6 (151).
Vewin, 2019. Drinking Water Fact Sheet 2019. Den Haag, the Netherlands.
Wang, Y., Sun, T., 2012. Life cycle assessment of CO2 emissions from wind power plants: Methodology and case studies. Renew. Energy 43, 30–36.
Yi, Y., Rao, A.D., Brouwer, J., Samuelsen, G.S., 2005. Fuel flexibility study of an integrated 25kW SOFC reformer system. J. Power Sources 144 (1), 67–76.
Zhang, L., Jiang, S.P., He, H.Q., Chen, X., Ma, J., Song, X.C., 2010. A comparative study of H2S poisoning on electrode behavior of Ni/YSZ and Ni/GDC anodes of solid oxide fuel cells. Int. J. Hydrogen Energy 35 (22), 12359–12368.
Zhou, C., Zheng, S., Chen, C., Lu, G., 2013. The effect of the partial pressure of H2S on the permeation of hydrogen in low carbon pipeline steel. Corrosion Sci. 67, 184–192.